10512 *Inorg. Chem.* **2010**, *49*, 10512–10521
DOI: 10.1021/ic101481c

Inorganic Chemistry
Article

Thermochemistry of Lewis Adducts of BH_3 and Nucleophilic Substitution of Triethylamine on NH_3BH_3 in Tetrahydrofuran

Robert G. Potter[†] and Donald M. Camaioni*

Pacific Northwest National Laboratory, P.O. Box 999, Richland, Washington 99352, United States

Monica Vasiliu and David A. Dixon*

Department of Chemistry, The University of Alabama, Tuscaloosa, Alabama 35487-0336, United States.
[†]Current address: Geophysical Laboratory, Carnegie Institution of Washington, Washington, D.C. 20005, U.S.A.

Received July 23, 2010

The thermochemistry of the formation of Lewis base adducts of BH_3 in tetrahydrofuran (THF) solution and the gas phase and the kinetics of substitution on ammonia borane by triethylamine are reported. The dative bond energy of Lewis adducts were predicted using density functional theory at the B3LYP/DZVP2 and B3LYP/6-311+G** levels and correlated ab initio molecular orbital theories, including MP2, G3(MP2), and G3(MP2)B3LYP, and compared with available experimental data and accurate CCSD(T)/CBS theory results. The analysis showed that the G3 methods using either the MP2 or the B3LYP geometries reproduce the benchmark results usually to within ~1 kcal/mol. Energies calculated at the MP2/aug-cc-pVTZ level for geometries optimized at the B3LYP/DZVP2 or B3LYP/6-311+G** levels give dative bond energies 2−4 kcal/mol larger than benchmark values. The enthalpies for forming adducts in THF were determined by calorimetry and compared with the calculated energies for the gas phase reaction: $THFBH_3 + L \rightarrow LBH_3 + THF$. The formation of NH_3BH_3 in THF was observed to yield significantly more heat than gas phase dative bond energies predict, consistent with strong solvation of NH_3BH_3. Substitution of NEt_3 on NH_3BH_3 is an equilibrium process in THF solution ($K \approx 0.2$ at 25 °C). The reaction obeys a reversible bimolecular kinetic rate law with the Arrhenius parameters: log $A = 14.7 \pm 1.1$ and $E_a = 28.1 \pm 1.5$ kcal/mol. Simulation of the mechanism using the SM8 continuum solvation model shows the reaction most likely proceeds primarily by a classical S_N2 mechanism.

Introduction

The study of Lewis acid/base complexes is of great importance to the fields of main group chemistry and organic synthesis.[1] Lewis-acidic boron compounds are particularly attractive because of low cost and environmental compatibility. They are used as catalysts in both olefin[2] and ring-opening[3] polymerizations and show promise as electrolyte additives for lithium-ion batteries.[4] More recently Lewis acid/base pairs have been used for the heterolytic cleavage of H_2[5] and complexation of CO_2[6]—two reactions fundamental to the field of energy conversion. The Lewis acids BH_3 and AlH_3 have been predicted to catalyze the elimination of H_2 from ammonia borane.[7] The thermochemistry of Lewis acid−base pairing has therefore received much attention. For example, we have predicted the Lewis acidities of a range of boron-containing Lewis acids based on their fluoride affinities and shown that the range of Lewis acidities is quite large and strongly dependent on the substituent.[8,9]

Lewis base (L) exchange reactions have been utilized as a strategy for the production of amine boranes,[10] most notably

*To whom correspondence should be addressed. E-mail: donald.camaioni@pnl.gov (D.M.C.), dadixon@bama.ua.edu (D.A.D.).

(1) Santelli, M.; Pons, J. M. *Lewis Acids and Selectivity in Organic Synthesis*; CRC Press: Boca Raton, FL, 1996.
(2) Sonnenschein, M. F.; Webb, S. P.; Redwine, D. O.; Wendt, B. L.; Rondan, N. G. *Macromolecules* **2006**, *39*, 2507.
(3) Shibasaki, Y.; Sanda, F.; Endo, T. *Macromolecules* **2000**, *33*, 3636.
(4) Zhang, S. S. *J. Power Sources* **2006**, *162*, 1379. Chen, Z. H.; Amine, K. *J. Electrochem. Soc.* **2006**, *153*, A1221. Chen, Z. H.; Liu, J.; Amine, K. *Electrochim. Acta* **2008**, *53*, 3267. Nair, N. G.; Blanco, M.; West, W.; Weise, F. C.; Greenbaum, S.; Reddy, V. P. *J. Phys. Chem. A* **2009**, *113*, 5918. Chang, C.-C.; Chen, T.-K.; Her, L.-J.; Fey, G. T.-K. *J. Electrochem. Soc.* **2009**, *156*, A828. Li, L. F.; Lee, H. S.; Li, H.; Yang, X. Q.; Huang, X. J. *Electrochem. Commun.* **2009**, *11*, 2296.
(5) Sumerin, V.; Shultz, F.; Nieger, M.; Leskelä, M.; Repo, T.; Rieger, B. *Angew. Chem., Int. Ed.* **2008**, *47*, 6001.
(6) Mömming, C. M.; Otten, E.; Kehr, G.; Fröhlich, R.; Grimme, S.; Stephan, D.; Erker, G. *Angew. Chem., Int. Ed.* **2009**, *48*, 6643.
(7) (a) Nguyen, M. T.; Nguyen, V. S.; Matus, M. H.; Gopakumar, G.; Dixon, D. A. *J. Phys. Chem. A* **2007**, *111*, 679. (b) Nguyen, V. S.; Matus, M. H.; Ngan, V. T.; Nguyen, M. T.; Dixon, D. A. *J. Phys. Chem. C* **2008**, *112*, 5662.
(8) Grant, D. J.; Dixon, D. A.; Camaioni, D.; Potter, R. G.; Christe, K. O. *Inorg. Chem.* **2009**, *48*, 8811.
(9) Christe, K. O.; Dixon, D. A.; McLemore, D.; Wilson, W. W.; Sheehy, J. A.; Boatz, J. A. *J. Fluor. Chem.* **2000**, *101*, 151.
(10) (a) Shore, S.; Chen, X. U.S. Patent 008160; (b) Baldwin, R.; Washburn, R. *J. Org. Chem.* **1961**, *26*, 3549. (c) Mittakanti, M.; Morse, K. W. *Main Group Met. Chem.* **1996**, *19*, 727. (d) Burnham, B. S. *Cur. Med. Chem.* **2005**, *12*, 1995.

Published on Web 10/08/2010

ammonia borane, which is a valuable reagent for organic synthesis[11] and a strong candidate for chemical hydrogen storage systems.[12] One major challenge remaining for the utilization of NH_3BH_3, as an on-board hydrogen fuel source for vehicles, is its regeneration from the spent, hydrogen-depleted, BNH_x materials produced from hydrogen release. Routes involving digestion to LBX_3 compounds that are subsequently converted to LBH_3 by hydrogenolysis or metathesis with hydride donors followed by displacement of L with ammonia have been demonstrated.[13,14] We have previously demonstrated the production of amine boranes from BX_3 compounds potentially derived from chemical digestion of spent NH_3BH_3 fuel with different HX reagents (X = OAr, SAr, F).[15] The B−N bond energies for NH_3BH_3 and for methyl substituted NH_3BH_3 on both B and C have been reliably predicted from high-level ab initio electronic structure calculations,[16,17] and there is additional work at a lower computational level on the effect of F atoms as a substituent.[18] Calculated gas phase B−N bond energies in methyl substituted NH_3BH_3 are in semiquantitative agreement with the experimental gas phase values.[19−21] Solution-phase calculations have received less attention despite the possibility of differential solvation energies between products and reactants and the wealth of solution-phase measurements available for comparison. For example, Flores-Segura and Torres[22,23] measured the enthalpies for forming pyridine and alkyl amine boranes in tetrahydrofuran (THF). The thermochemistry and kinetics of reactions in THF are particularly important because of the wide variety of chemical reactions that can be conducted in this solvent. Whereas amine exchange reactions involving aryl amines and BH_3 appear to be rapid,[24] reactions involving alkyl amines are slow.[25−27] To our knowledge measurements of the rates and activation barriers of intermolecular amine exchange reactions involving NH_3BH_3 have not been reported.

Herein we extend measurements of the enthalpies for forming B−N bonds to BH_3 in THF and thermochemical kinetic parameters for triethylamine-ammonia exchange on BH_3 in THF. Complementing these results, we used density functional theory (DFT) and molecular orbital (MO) theory to calculate these same parameters to test the predictive value of currently available methods and to better understand the reaction mechanism. We performed calculations on adducts of borane for selected amines and other bases to improve our understanding of the effects of structure on the dative bond strength. We used continuum solvation models based on the self-consistent reaction field approach (SCRF)[28] to simulate the mechanism for triethylamine-ammonia exchange on BH_3 in THF solution. The results show that the SM8 continuum solvation models can be used to predict, with near chemical accuracy, the thermochemistry and activation parameters in THF. Thus, on the basis of experiment and theory, we conclude that the reaction proceeds primarily by a classical S_N2 mechanism.

Results and Discussion

Gas Phase Thermochemistry of Lewis Base BH_3 Adducts. The gas phase binding energies of borane with a variety of Lewis bases calculated at the DFT (B3LYP/6-311+G** or B3LYP/DZVP2) level and with correlated MO methods up to the CCSD(T) level are shown in Table 1 for reaction 1:

$$L(g) + BH_3(g) \rightarrow LBH_3(g) \qquad (1)$$

Available experimental values in kcal/mol are as follows: NH_3BH_3 31.0 ± 2.6,[29] $MeNH_2$ 32.8 ± 1.3,[30] Me_2NH 34.5 ± 0.7,[30] Me_3N 38.2 ± 0.2,[30] and Me_2S 25.8.[31] The values are in accord with calculations at the CCSD(T)/CBS (complete basis set) and G3MP2 levels of theory (see ref 17 and Table 1). The energies obtained from DFT with the B3LYP functional are significantly different from the results from correlated methods. The failure of DFT to predict BN bond energies has been noted elsewhere.[18] Although DFT underestimates the increase in the B−N dative bond energy with degree of N-alkylation, the optimized DFT and MP2 geometries agree to within 0.02 Å.[18,32] Therefore, we performed calculations using the G3B3LYP-(MP2) and MP2/aug-cc-pVTZ//DFT model chemistries to compare with G3(MP2) and CCSD(T)/CBS models that use more time-consuming MP2 geometry optimization steps and for CCSD(T)/CBS much larger basis sets at the CCSD(T) level. Dative bond energies calculated in this way are 2−4 kcal/mol larger than benchmark CCSD(T)/CBS

(11) Andrews, G. C. Borane−Ammonia. In *Encyclopedia of Reagents for Organic Synthesis*; Paquette, L., Ed.; John Wiley & Sons: New York, 2004.
(12) Stephens, F. H.; Pons, V.; Baker, R. T. *Dalton Trans.* **2007**, *25*, 2613.
(13) (a) Ramachandran, P. V.; Gagare, P. D. *Inorg. Chem.* **2007**, *46*, 7810. (b) Hausdorf, S.; Baitlalow, F.; Wolf, G.; Mertens, F. *Int. J. Hydrogen Energy* **2008**, *33*, 608.
(14) Davis, B. L.; Dixon, D. A.; Garner, E. B.; Gordon, J. C.; Matus, M. H.; Stephens, F. H. *Angew. Chem.* **2009**, *48*, 6812.
(15) (a) Mock, M. T.; Potter, R. G.; Camaioni, D. M.; Li, J.; Dougherty, W. G.; Kassel, W. S.; Twamley, B.; DuBois, D. L. *J. Am. Chem. Soc.* **2009**, *131*, 14454. (b) Camaioni, D. M.; Heldebrant, D. J.; Linehan, J. C.; Shaw, W. J.; Li, J.; DuBois, D. L.; Autrey, T. *Prepr. Pap. Am. Chem. Soc., Div. Fuel Chem.* **2007**, *52*, 509.
(16) Gutowski, M.; Dixon, D. A. *J. Phys. Chem. A* **2005**, *109*, 5129.
(17) Grant, D. J.; Matus, M. H.; Anderson, K. D.; Camaioni, D. M.; Neufeldt, S.; Lane, C. F.; Dixon, D. A. *J. Phys. Chem. A* **2009**, *113*, 6121.
(18) Gilbert, T. M. *J. Phys. Chem. A.* **2004**, *108*, 2550.
(19) Haaland, A. *Angew. Chem., Int. Ed. Engl.* **1989**, *28*, 992.
(20) McCoy, R. E.; Bauer, S. H. *J. Am. Chem. Soc.* **1956**, *78*, 2061.
(21) Aldridge, S.; Downs, A. J.; Tang, C. Y.; Parsons, S.; Clarke, M. C.; Johnstone, R. D. L.; Robertson, H. E.; Rankin, D. W. H.; Wann, D. A. *J. Am. Chem. Soc.* **2009**, *131*, 2231.
(22) Flores-Segura, H.; Torres, L. A. *Struct. Chem.* **1996**, *7*, 363.
(23) Flores-Segura, H.; Torres, L. A. *Struct. Chem.* **1997**, *8*, 227.
(24) Camacho, C.; Paz-Sandoval, M. A.; Contreras, R. *Polyhedron* **1986**, *5*, 1723.
(25) Ryschkewitsch, G. E.; Cowley, A. H. *J. Am. Chem. Soc.* **1970**, *92*, 745.
(26) Hawthorne, M. F.; Budde, W. L. *J. Am. Chem. Soc.* **1971**, *93*, 3147.
(27) Toyota, S.; Futawaka, T.; Asakura, M.; Ikeda, H.; Oki, M. *Organometallics* **1998**, *17*, 4155.
(28) Tomasi, J.; Mennucci, B.; Cammi, R. *Chem. Rev.* **2005**, *105*, 2999.
(29) (a) Uses ΔH_f° = 36.6 ± 2.4, 11.0 ± 0.1, and 25.5 kcal/mol for NH_3BH_3(s),[29b] NH_3(g),[29c] BH_3(g),[29c] respectively, and ΔH_{sub}° NH_3BH_3 = 20.12 ± 0.05 kcal/mol.[58] (b) Baumann, J. Ph.D. Dissertation, TU Bergakademie Freiberg, Germany, 2003; Wolf, G. *W. E.-Heraeus-Seminar on Hydrogen Storage with Novel Nanomaterials*; Bad Honnef, Germany, October 23−27, 2005 (http://www.h-workshop.uni-konstanz.de/pdf/Wolf_Gert.pdf). (c) Linstrom, P. J.; Mallard, W. G., Eds.; *NIST Chemistry WebBook*, NIST Standard Reference Database Number 69, June 2005; National Institute of Standards and Technology: Gaithersburg, MD (http://webbook.nist.gov/chemistry/).
(30) From calorimetry data of McCoy and Bauer[20] on the reaction of diborane with methylated amine boranes using ΔH° = 41 kcal/mol for dissociation of diborane,[16,29c] and ΔH_{sub}° reported by: Alton, E. R.; Brown, R. D.; Carter, J. C.; Taylor, R. C. *J. Am. Chem. Soc.* **1959**, *81*, 3550; See also ref 21.
(31) Reference 41 reevaluated with current dissociation enthalpy for B_2H_6.[16,29c]
(32) Plumley, J. A.; Evanseck, J. D. *J. Phys. Chem. A* **2007**, *111*, 13472.

Table 1. Gas Phase Binding Energies ($-\Delta H°$) of Select Lewis Bases (L) with BH_3 Calculated at Various Levels of Theory at 298 K

	B3LYP					
ligand, L	6-311+G**	DZVP2	MP2[a]	G3MP2	CCSD(T)/CBS	BH_3-L μ (D)
NH_3	25.1	25.2	29.6	27.7 (27.6)[b]	27.7[c,d]	5.48
$MeNH_2$		27.2		31.1	33.4[d]	5.39
n-$PrNH_2$		30.1		33.7		5.90
s-$BuNH_2$		28.9		33.1		5.84
CH_2=$CHCH_2NH_2$		29.1		33.1		5.67
$NH_2(CH_2)_2NH_2$		28.9		32.8		4.39
$NH_2(CH_2)_2NH_2BH_3$		26.3		30.0		0.00
1,2-diaminocyclohexane		32.5		36.0		7.16
1,2-diaminocyclohexane BH_3		25.9		30.8		7.52
1,3-diaminocyclohexane		28.8		32.9		7.07
1,3-diaminocyclohexane BH_3		26.7		31.0		10.50
1,4-diaminocyclohexane		27.5		31.8		4.24
1,4-diaminocyclohexane BH_3		27.0		31.3		0.00
2,6-dimethylpiperidine		26.0		32.6		5.48
Me_2NH		31.1		36.9	36.7[d]	5.38
MeEtNH		30.2		36.1		5.29
Et_2NH		28.7		35.0		5.17
piperidine		32.5		38.0		6.00
NMe_3	28.6	30.4	41.6	38.0	37.8[d]	5.20
NEt_3	24.2	26.7	39.5	35.9 (36.7)[b]		5.03
$PhNH_2$		21.4		26.3		5.18
2,6-Me_2PhNH_2		21.7		26.8		4.84
$PhNMe_2$		21.0		28.3		4.86
$PhNEt_2$		22.7		31.9		4.74
4-dimethylaminopyridine (DMAP)		32.2		35.3		10.19
NPh_3	2.3	5.6	22.0	17.6		4.37
pyridine	27.8	29.6	36.1	33.4		6.67
2,6-lutidine	20.5	26.1	34.4	30.8		5.52
PH_3	17.7	18.4	25.1	22.1	22.5[c]	4.37
PMe_3		32.6		38.3		5.43
PEt_3	31.0	32.5	42.4	39.1		5.20
PPh_3	27.3	29.2	40.4	35.2		5.24
$P(OMe)Me_2$		33.4		40.1		3.90
$P(OMe)_2Me$		32.2		39.8		2.76
$P(OMe)_3$		30.9		40.0		1.49
AsH_3	12.1[e]	11.3[f]	21.8 (20.4)[g]		15.7	3.91
$AsEt_3$	21.9[e]	22.3[f]	25.7 (32.7)[g]		28.0[h]	5.07
$AsPh_3$	14.6[e]	19.9[f]	33.5 (26.8)[i]		23.0[h]	5.18
Me_2S	17.7	19.8	27.9	25.3		4.87
Et_2S		20.4		26.1		4.79
Ph_2S		14.8		20.9		5.05
Me_2O		14.9		19.8		4.87
THF	15.8	16.7	24.3	21.4 (21.1)[b]		5.74
Et_2O	10.8	12.1	20.5	17.7		4.72

[a] MP2/aug-pVTZ//B3LYP/6-311+G**. [b] G3(MP2)B3. [c] ref 16. [d] ref 17. [e] Ahlrichs VTZ basis set on As. [f] DZVP Basis set on all atoms. [g] aug-cc-pVTZ-PP on As. [h] Calculated by an isodesmic reaction at the MP2 level relative to the CCSD(T)/CBS value for AsH_3:BH_3. [i] aug-cc-pVDZ-PP on As, aug-cc-pVDZ on C and H.

values due in part to basis set superposition error (BSSE).[32] To illustrate this point, we estimated by counterpoise[33] calculation that the bond energy of NH_3BH_3 at the MP2/aug-cc-pVTZ//B3LYP/6-311+G** level is too large by 2.5 kcal/mol. In general, nitrogen and phosphorus bases were calculated to be the strongest donors with average B−L bond lengths of 1.65 and 1.95 Å, respectively, whereas oxygen, sulfur, and arsenic-containing bases were among the weakest. These results are consistent with experimentally observed trends for a range of Lewis acids.[34] Alkyl and aryl groups attached to the donor atom increase the strength of the Lewis base relative to H with aryl substitution being less effective than alkyl.[35]

Experimental Thermochemistry for Lewis-Base Exchange with BH_3 in THF. Select bases from the computational study were investigated experimentally to determine the enthalpy of reaction with BH_3 in THF. The experiment measures the enthalpy for the exchange reaction 2.

$$THFBH_3(soln) + L(soln) \rightarrow LBH_3(soln) + THF(l) \quad (2)$$

In general, strong acid base pairs (NH_3BH_3, Et_3PBH_3, pyridine BH_3, etc.) were found to be stable, whereas the weaker pairs (THFBH_3, Me_2SBH_3, 2,6-lutidine BH_3, etc.) would slowly decompose after prolonged storage at room temperature in ambient atmosphere. Enthalpies for forming adducts are listed in Table 2 together with data from Flores-Segura and Torres[22,23] to complement/supplement our determinations for NH_3 and other Lewis bases.

(33) Boys, S. F.; Bernardi, F. *Mol. Phys.* **1970**, *19*, 553.
(34) Stone, F. G. A. *Chem. Rev.* **1958**, *58*, 101, and references therein.
(35) Planar Ph_3N is known to have an unusually low Brønsted basicity: Hoefnagel, A. J.; Hoefnagel, M. A.; Wepster, B. M. *J. Org. Chem.* **1981**, *46*, 4209, and is the one anomaly to this trend.

Table 2. Experimental Enthalpies (kcal/mol) for Reaction of Lewis Bases with 0.5 M $THFBH_3$ in THF Solution and Calculated Gas Phase Reaction Enthalpies[a]

L	$-\Delta H_2°$ soln	$-\Delta H_2°$ gas[b]
NH_3	14.9 ± 0.1	6.3
NH_2Pr	19.1 ± 0.5[c]	12.3
$NHEt_2$	16.9 ± 0.3[c]	13.6
NEt_3	14.6 ± 0.1 14.5 ± 0.1[c]	14.5
NPh_3	no exotherm	−3.8
pyridine	12.7 ± 0.3[d] 14.6[e]	12.0
lutidine	5.4 ± 0.5[d]	9.4
PEt_3	16.6 ± 0.3	17.7
PPh_3	12.4 ± 0.3	13.8
SMe_2	3.3 ± 0.1	3.9

[a] Conditions: 5 vol % Lewis base/THF and 0.5 M $THFBH_3$ at 25 °C, unless noted. [b] $\Delta H_1(THF) - \Delta H_1(L)$ from Table 1 using G3MP2 results. [c] Values for reaction of 0.1 M $THFBH_3$ with dilute solutions of amine.[23] [d] Run in 50 vol% Lewis base/THF solution. [e] Value for pyridine in dilute solution.[22]

From Table 1, the gas phase binding energy of THF to BH_3 is calculated to be ~21 kcal/mol at the G3MP2 level. To evaluate the effects of solvation, we compare in Table 2 the enthalpies for reaction 2 with the values, $\Delta H_2(gas) = \Delta H_1(THF) - \Delta H_1(L)$, from G3MP2 data in Table 1. The difference, ΔH_2 soln − ΔH_2 gas, corresponds to the differential solvation of products and reactants. It can be seen that ΔH_2 soln deviates from ΔH_2 gas in some cases, notably NH_3 and NH_2Pr. Thus, although alkyl amines bind BH_3 more strongly than NH_3 in the gas phase, solvation in THF counters this trend. Differential solvation effects are evident to a lesser extent for the adduct of *n*-Et_2NH but not of Et_3N. NH_3BH_3 has a large dipole (4.9 and 5.2 D in dioxane solution and in the gas phase, respectively)[36,37] as do many other amine boranes (Table 1), but its smaller size enhances electrostatic interaction with THF.[38] Brønsted basicities of amines have been shown to have a strong solvent dependence and the large difference in the gas phase basicities is substantially compressed in solution.[39,40]

The reactions of pyridine and lutidine with $THFBH_3$ are affected differently in solution, too. The reactions in the gas phase are exothermic by 12 and 10 kcal/mol, respectively. Reaction 2 with lutidine is much less favorable than with pyridine, so much so, that lutidine had to be added in large excess to shift the equilibrium to >98% conversion for accurate measurement of the resulting exotherm. A 5 kcal/mol exotherm was observed in the lutidine reaction compared to a 13 kcal/mol exotherm for pyridine recorded at the same (~4 M) concentrations. For purposes of comparison, these reactions were run at concentrations where pyridine and lutidine were effectively cosolvents. Thus, some of this difference could be due to solvent properties of these mixed solvents.

Differential solvation effects are smaller in the case of Et_3P and Ph_3P. The difference, ΔH_2 soln − ΔH_2 gas, is less than 2 kcal/mol. Graham and Stone[41] showed that the ligand exchange reaction of trimethylphosphines with trimethylamine borane (Me_3NBH_3) is reversible in the gas phase with $\Delta G_o = -1.7$ kcal/mol at 120 °C. Comparable results were observed by Shore and co-workers for the equilibrium in glyme or THF solutions.[42] These observations are consistent with the enthalpies we have calculated for forming BN and BP bonds in the gas phase ((Table 1) and determined in THF solution (Table 2). In contrast to the similarity of BN and BP bond energies in fully methylated amine and phosphine borane systems, the difference in gas phase bond energies of BH_3NH_3 and BH_3PH_3 is 5.2 kcal/mol (CCSD(T)/CBS level) with the B−N bond energy being larger.[16,17,43]

Consistent with the predicted gas phase values, reactions with O and S bases were too weak to be measured in most cases. When a large excess of SMe_2 was used, complete conversion to Me_2SBH_3 was observed accompanied by a modest (3 kcal/mol) exotherm. Being the same as the G3MP2 gas phase value for reaction 2, we conclude in this case that differential solvation is negligible.

Thermodynamics and Kinetics of Triethylamine/Ammonia Exchange in THF. The similarity in ΔH_2 soln (Table 2) for NH_3BH_3 and Et_3NBH_3 suggests that ammonia-triethylamine exchange of borane (3) may be a reversible process at ordinary temperatures in THF.

$$Et_3N + NH_3BH_3 \leftrightarrows H_3N + Et_3NBH_3 \qquad (3)$$

Therefore, we measured equilibrium and rate constants for the reaction using ^{11}B NMR. Figure 1 shows a stacked plot of NMR spectra recorded for a reaction run at 35 °C. The reactions were carried out in flame-sealed NMR tubes to ensure that reagents did not diffuse out of the tubes over the course of the reaction. Also, the tubes were filled with solution to minimize the headspace volume such that the fraction of NH_3 in the gas phase was negligible and the solution concentration of NH_3 could be estimated from the reaction stoichiometry. Reactions were run using 0.03−0.1 M NH_3BH_3 and 0.3−1.5 M Et_3N. Under these conditions, the reactions reached equilibrium with ~70% of NH_3BH_3 converted to Et_3NBH_3. Reaction rates increased significantly with temperature while changes in the equilibrium constant with temperature were small. Reactions took longer than 30 days to attain equilibrium at room temperature, but were completed within a day at 50 °C under the dilute (0.06 M) concentrations. Negligible decomposition of NH_3BH_3 by loss of hydrogen[44] was observed in the 23−50 °C temperature range of the current study. The initial rates for conversion of NH_3BH_3 into Et_3NBH_3 at 35 °C depended on the concentrations of both NH_3BH_3 and Et_3N. Therefore, the kinetic data were fit using non-linear regression (Levenberg−Marquardt algorithm)[45] of the numerically integrated rate equation for the reversible bimolecular reaction 3. The results

(36) Weaver, J. R.; Shore, S. G.; Parry, R. W. *J. Chem. Phys.* **1958**, *29*, 1.
(37) (a) Suenram, R. D.; Thorne, L. R. *Chem. Phys. Lett.* **1981**, *78*, 157. (b) Thorne, L. R.; Suenram, R. D.; Lovas, F. J. *J. Chem. Phys.* **1983**, *78*, 167.
(38) For example, the Bell and Onsager models for solvation of a point dipole in a spherical cavity show the solvent reaction field decreases with increasing size of the cavity: Bell, R. P. *J. Chem. Soc. Faraday Trans.* **1931**, *27*, 797. Onsager, L. *J. Am. Chem. Soc.* **1936**, *58*, 1486.
(39) (a) Headley, A. D. *J. Org. Chem.* **1991**, *56*, 3688. (b) Arnett, E. M.; Jones, F. M.; Taagepera, M.; Henderson, J. L.; Beauchamp, J. L.; Holtz, D.; Taft, R. W. *J. Am. Chem. Soc.* **1972**, *94*, 4724.
(40) Rõõm, E.-I.; Kütt, A.; Kaljurand, I.; Koppel, I.; Leito, I.; Koppel, I. A.; Mishima, M.; Goto, K.; Miyahara, Y. *Chem.—Eur. J.* **2007**, *13*, 7631.
(41) Graham, W. A. G.; Stone, F. G. A. *J. Inorg. Nuc. Chem.* **1956**, *3*, 164.
(42) Young, D. E.; McAchran, G. E.; Shore, S. G. *J. Am. Chem. Soc.* **1966**, *88*, 4390.
(43) Grant, D. J.; Dixon, D. A. *J. Phys. Chem. A.* **2005**, *109*, 10138.
(44) Shaw, W. J.; Linehan, J. C.; Szymczak, N. K.; Heldebrant, D. J.; Yonker, C.; Camaioni, D. M.; Baker, R. T.; Autrey, T. *Angew. Chem., Int. Ed.* **2008**, *47*, 7493.
(45) Press, W. H.; Flannery, B. P.; Teukolsky, S. A.; Vetterling, W. T. *Numerical Recipes - the Art of Scientific Computing*; 2nd ed.; University Press: Cambridge, 1992.

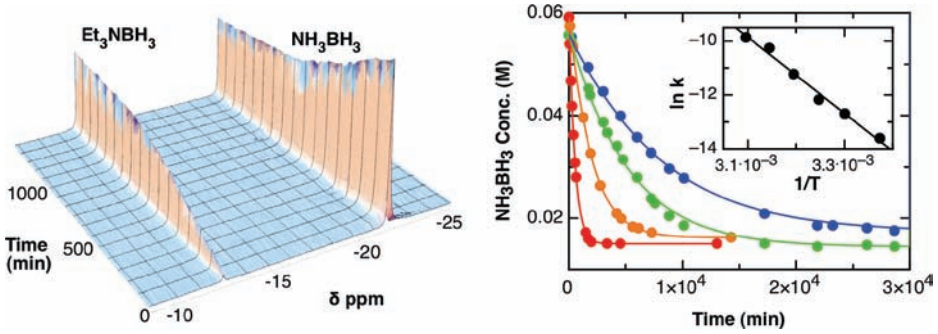

Figure 1. (left) Time-resolved ^{11}B NMR stacked spectra of the reaction of Et_3N with NH_3BH_3 in THF at 45 °C; (right) fit of kinetic data to reversible second order rate law at (blue) 30°, (green) 35°, (orange) 40°, and (red) 50 °C; (inset) data fit to Arrhenius equation.

Table 3. Rate and Equilibrium Constants Measured for Reaction: $NEt_3 + NH_3BH_3 \leftrightarrows NEt_3BH_3 + NH_3$[a]

T °C	$[Et_3N]_0$	$[NH_3BH_3]_0$	$[NH_3BH_3]_{eq}$	k ($\times 10^6$) M^{-1} s^{-1}	K_{eq}
23.5[b]	0.402	0.0276	0.0173	1.11	0.199
30.0	0.430	0.0557	0.0173	3.17	0.218
35.0	0.430	0.0557	0.0144	5.54	0.304
35.0	1.395	0.0338	0.00308	4.40	0.225
40.0	0.431	0.0590	0.0162	13.0	0.291
45.0	0.287	0.1020	0.0455	35.0	0.304
50.0	0.431	0.0592	0.0150	52.4	0.337

[a] Uncertainties in rates are ~2% except for the rate at 23.5 °C, for which the uncertainty is 5%. [b] This reaction had initial concentrations of $[NH_3] = [Et_3NBH_3] = 0.028$ M.

are shown in Figure 1 and tabulated in Table 3. Also shown in Figure 1, is an Arrhenius analysis of the bimolecular rate constant for conversion of NH_3BH_3 into Et_3NBH_3 for the range of 23°−50 °C (see Figure 1 inset), giving log $A = 14.7 \pm 1.1$ and $E_a = 28.1 \pm 1.5$ kcal/mol. The corresponding $\Delta G^{\ddagger}$ is 27 ± 2 kcal/mol and $\Delta S^{\ddagger}$ is 6.7 ± 0.3 cal/mol·K. The $\Delta G_r°$ ~ 1 kcal/mol at 25 °C decreases to ~0.7 kcal/mol at 50 °C; therefore, $\Delta S_r°$ is positive and small.

The $\Delta S^{\ddagger}$ is opposite in sign compared to what may be expected. For example, Hawthorne and Budde[26] determined that S_N2-type substitution on Me_3NBH_3 by tri-*n*-butylphosphine in dichlorobenzene solvent has $\Delta S^{\ddagger} = -5 \pm 3$ cal/mol·K. A positive $\Delta S^{\ddagger}$ for substitution on NH_3BH_3 requires the transition state (TS) to be less well solvated than reactants, in which case the solvent may gain enough entropy to offset the loss of entropy by the reactants in forming the TS. This seems plausible given that the dipole moment for NH_3BH_3 is large.[36,37] In what follows, we consider the mechanism and the solvation effects on the reaction in more detail.

The competition between the S_N1 and S_N2 mechanisms for substitution on NH_3BH_3 has previously been addressed computationally. Czerw et al.[46] calculated the structure and bonding in the hyper-coordinated *bis*-ammonia borane adduct, which is a TS for the S_N2 identity reaction of NH_3BH_3. They estimated the barrier to be 11.1−12.8 kcal/mol at electron-correlated levels of theory including MP4(SDTQ), QCISD(T), and CCSD(T) and the G2 and CBS-Q methods. Toyota et al.[47] modeled the S_N1 and S_N2 mechanisms of NH_3 substitution on NH_3BH_3 and concluded that free energies of activation for the two pathways are comparable at 300 K in the vacuum. Ziegler and co-workers[48] followed with ab initio (DFT) molecular dynamics calculations of the free energy surface of the same reaction. They found that the S_N2 mechanism is favored at 300 K, but at 600 K the reaction appeared to follow an S_N1 mechanism because of entropy effects. How solvent may affect the competition is unclear. We also considered a competing 2-step pathway involving sequential S_N2 reactions in which BH_3 is transferred from ammonia to THF followed by transfer from THF to NEt_3 as shown in reactions 4 and 5. While individual kinetic runs could be fit to the scheme by numerical integration of the differential rate equations, we discount this mechanism because the data sets for 0.4 and 1.4 M NEt_3 at 35 °C could not be fit by the same set of rate constants. To elucidate the mechanism and solvent effects, we modeled reaction 3−5 as discussed in the next section.

$$H_3NBH_3 + THF \leftrightarrows NH_3 + THFBH_3 \qquad (4)$$

$$Et_3N + THFBH_3 \leftrightarrows Et_3NBH_3 + THF \qquad (5)$$

Solution Modeling. We used electronic structure theory to calculate the NH_3/NEt_3 substitution reactions in the gas and THF solution phases. We used continuum solvation models using the SCRF approach because they are computationally efficient and reliable for simulating effects of solvation.[28,49] These models do have potential issues with the description of the entropy component of the rate expression because of lack of inclusion of solvent rearrangement effects, especially cavity formation. As standard free energies of solvation (ΔG_s*) are not available for amine boranes, we use the thermochemistry we measured for reaction 3 (vide supra) to benchmark select continuum solvation models. Then, we modeled the competing 2-step pathway that occurs by sequential S_N2 reactions in which BH_3 is transferred from ammonia to THF followed by transfer from THF to NEt_3 as shown in reactions 4 and 5.

(46) Czerw, M.; Goldman, A. S.; Krogh-Jespersen, K. *Inorg. Chem.* **2000**, *39*, 363.
(47) Toyota, S.; Futawaka, T.; Asakura, M.; Ikeda, H.; Ōki, M. *Organometallics* **1998**, *17*, 4155.
(48) Yang, S.-Y.; Fleurat-Lessard, P.; Hristov, I.; Ziegler, T. *J. Phys. Chem. A* **2004**, *108*, 9461.
(49) Cramer, C. J.; Truhlar, D. G. *Acc. Chem. Res.* **2008**, *41*, 760.

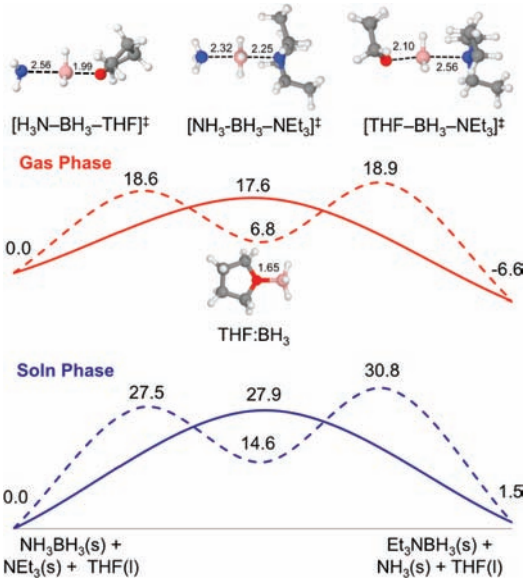

Figure 2. (top) Gibbs free energy diagram calculated for 1- and 2-step substitution reactions at the G3(MP2)B3LYP level of theory; (bottom) diagram for reactions in THF solution at SM8/B3LYP/6-31G*//G3-(MP2)B3LYP; energies in kcal/mol and bond distances in Å. Reactants are 17.5 kcal/mol more stable in solution phase.

The equilibrium of diborane gas with $THFBH_3$ in liquid THF provides another benchmark for the solvation models. Elliot et al.[50] reported the vapor pressure and solubility of diborane over the temperature range of 280−323 K. Thus, with $\Delta G^\circ = 40$ kcal/mol for the gas phase bond energy of diborane, $\Delta G_6^\circ = -16.1$ kcal/mol can be estimated (See Supporting Information, Scheme S1). Below we will compare this value to the calculated value obtained using G3MP2B3LYP theory to estimate the BE of $THFBH_3$ (Table 1) and the calculated solvation free energies of THF and $THFBH_3$.

$$BH_3(g) + THF(l) \rightarrow THFBH_3(soln) \qquad (6)$$

Reactants, products, and transition states were modeled in the gas phase at the G3(MP2)B3LYP level of theory. The lowest energy structures of TSs and $THFBH_3$ are shown at the top of Figure 2. Additional structures and their energies are in the Supporting Information. The G3(MP2)B3LYP method optimizes the geometry at the B3LYP/6-31G* level. At this level, the B−N distances in the S_N2 TS are 2.323 and 2.251 Å to ammonia and NEt_3 portions of the structure compared to 1.668 and 1.670 Å in NH_3BH_3 and Et_3NBH_3, respectively. To calculate standard solvation free energies (ΔG_s^*),[51] we used the SM8 model[52] implemented in GAMESSPLUS,[53] the SSC(V)PE model[54] implemented in HONDO 2006,[55] and the COSMO models[56] as implemented in the Gaussian 03[57] and Amsterdam Density Functional (ADF)[58] programs. The methods differ in their definitions of the solute cavity, calculation of the electrostatic contribution to solvation (interaction of solute with bulk dielectric), and in the estimation of non-electrostatic contributions to solvation (formation of solute cavity, dispersion and repulsion interactions of solute with solvent). The SSC(V)PE model defines the cavity to be the 0.001 e^-/bohr^3 isodensity contour of the molecule in the vacuum to calculate the electrostatic contribution to the solvation free energy. It does not include a non-electrostatic contribution, so, it may only be useful when these contributions are small or will cancel in calculating reaction free energies. However, use of this contour has been found to reproduce solution properties for a wide variety of molecules and to consistently predict acidities of organic acids in aprotic solvents.[59] The SM8 model is based on a generalized Born model of solvation[60,61] with inclusion of non-electrostatic effects due to cavity formation, dispersion interactions, and changes in solvent structure denoted in SM8 as G-CDS. The COSMO models also predict electrostatic and non-electrostatic contributions to solvation and use the Conductor-like Screening Model[56] to calculate the electrostatic component. The SM8 model has been systematically parametrized for a wide variety of solvents and tends to give consistently good results for neutral solutes in a variety of solvents.[52] The COSMO model has been widely used and provides good solvation estimates and *even* boiling points in the COSMO-RS[56,62] formalism.

The calculated ΔG_s^* values are listed in Table 4. The lack of reliable Henry's law constants for the compounds in THF prevents comparison of ΔG_s^* with experiment for individual compounds, except THF ($\Delta G_s^* = -4.3$ kcal/mol)[63] and $THFBH_3$ ($\Delta G_s^* = -8.5$ kcal/mol).[64] In these cases, the SM8 model results are in agreement with experiment. Except for NH_3, the SSC(V)PE model obtains less negative values of ΔG_s^* as expected since it calculates only the electrostatic contribution to solvation. The models are generally in agreement with each other with respect to the electrostatic contributions to solvation differing by ~1 kcal/mol except in the case of NH_3BH_3 for

(50) Elliott, J. R.; Roth, W. L.; Roedel, G. F.; Boldebuck, E. M. *J. Am. Chem. Soc.* **1952**, *74*, 5211.
(51) Ben-Naim, A.; Marcus, Y. *J. Chem. Phys.* **1984**, *81*, 2016.
(52) (a) Marenich, A. V.; Olson, R. M.; Kelly, C. P.; Cramer, C. J.; Truhlar, D. G. *J. Chem. Theory Comput.* **2007**, *3*, 2011. (b) Cramer, C. J.; Truhlar, D. G. *Acc. Chem. Res.* **2008**, *41*, 760.
(53) Higashi, M. et al. *GAMESSPLUS*, version 2010; University of Minnesota: Minneapolis, MN, 2010.
(54) Chipman, D. M. *J. Chem. Phys.* **2002**, *116*, 10129.
(55) Dupuis, M.; Marquez, A.; Davidson, E. R. *HONDO*, ver. 06.10, 2006, based on HONDO 95.3. Dupuis, M.; Marquez, A.; Davidson, E. R. Quantum Chemistry Program Exchange (QCPE), Indiana University: Bloomington, IN 47405.
(56) Klamt, A.; Schümann, G. *J. Chem. Soc., Perkin Trans. 2* **1993**, 799. Klamt, A. *Quantum Chemistry to Fluid Phase Thermodynamics and Drug Design*; Elsevier: Amsterdam, 2005.
(57) Frisch, M. J. et al. *Gaussian 03*, Revision E.01; Gaussian, Inc.: Wallingford, CT, 2004.
(58) (a) Baerends, E. J. et al. *ADF2008.01*; SCM, Vrije Universiteit: Amsterdam, The Netherlands, 2008; http://www.scm.com. (b) Fonseca Guerra, C.; Snijders, J. G.; te Velde, G.; Baerends, E. J. *Theor. Chem. Acc.* **1998**, *99*, 391. (c) te Velde, G.; Bickelhaupt, F. M.; van Gisbergen, S. J. A.; Fonseca Guerra, C.; Baerends, E. J.; Snijders, J. G.; Ziegler, T. *J. Comput. Chem.* **2001**, *22*, 931.
(59) (a) Zhan, C.-G.; Chipman, D. M. *J. Chem. Phys.* **1999**, *110*, 1611. (b) Zhan, C.-G.; Chipman, D. M. *J. Chem. Phys.* **1998**, *109*, 10543. (c) Chipman, D. M. *J. Phys. Chem. A* **2002**, *106*, 7413.
(60) Bashford, D.; Case, D. A. *Annu. Rev. Phys. Chem.* **2000**, *51*, 129.
(61) Cramer, C. J. *Essentials of Computational Chemistry*, 2nd ed.; John Wiley & Sons Ltd.: Chichester, 2004.
(62) Klamt, A.; Jonas, V.; Bürger, T.; Lohrenz, J. C.W. *J. Phys. Chem. A* **1998**, *102*, 5074.
(63) $\Delta G_s^* = -4.3$ kcal/mol for 8.72×10^{-3} M vapor to change into 12.2 M liquid at 298 K; concentrations determined from density (0.883 g/mL) of the liquid and its vapor pressure (0.2134 atm): Aminabhavi, T. M.; Gopalakrishna, B. *J. Chem. Eng. Data* **1995**, *40*, 856.
(64) (a) Derived from thermochemical cycle (Supporting Information, Scheme S1) using literature data[64b] for equilibrium concentration of diborane over BH_3 in THF solution and standard state correction, $\Delta G_s^* = -\Delta G_{vap}^\circ - 1.9$ kcal/mol. (b) Elliott, J. R.; Roth, W. L.; Roedel, G. F.; Boldebuck, E. M. *J. Am. Chem. Soc.* **1952**, *74*, 5211.

Table 4. Standard Free Energies of Solvation (ΔG_s*) in kcal/mol Calculated Using Continuum Solvation Models

		SM8[b]			COSMO G03[d]			COSMO ADF[e]		
compound	SSC(V)PE[a]	electro-static	non-electrost.[c]	total	electro-static	non-electrost.	total	electro-static	non-electrost.	total
ammonia (C_{3v})	−4.2	−4.2	1.1	−3.1	−5.5	1.7	−3.8	−5.1	1.4	−3.7
ammonia Borane (C_{3v})	−12.6	−15.6	−1.2	−16.8	−15.0	4.4	−10.6	−15.6	1.6	−14.0
triethylamine (C_3)	−1.2	−1.3	−2.3	−3.6	−2.1	6.1	4.0	−1.4	2.2	0.8
$[H_3NBH_3NEt_3]^‡$ (C_1)	−5.2	−7.2	−1.1	−8.3	−6.2	11.2	5.0	−6.0	2.4	−3.6
triethylamine Borane (C_1)	−6.1	−8.3	−0.9	−9.2	−8.8	8.1	−0.7	−8.5	2.2	−6.3
tetrahydrofuran (C_2)[f]	−2.4	−1.3	−3.1	−4.4	−4.3	3.1	−1.3	−4.3	1.8	−2.5
tetrahydrofuran Borane (C_1)[f]	−6.6	−8.0	−0.8	−8.8	−8.8	6.1	−2.7	−8.5	2.0	−6.5

[a] SSC(V)PE-isodensity/B3LYP/6-31G*//B3LYP/6-31G*; electrostatic only. [b] SM8/B3LYP/6-31G*//B3LYP/6-31G*. [c] Sum of cavity, dispersion, and changes in solvent structure corrections to SM8 model. [d] COSMO model in Gassian03 using B3LYP/DZVP2 level of theory. [e] COSMO model in ADF at the B88P86/TZ2P level of theory. [f] Experimental values: THF, −4.3; $THFBH_3$, −8.5 (see Supporting Information, Scheme S1).

Table 5. Standard Free Energies (kcal/mol) of Reaction and Activation in Solution Calculated Using Continuum Solvation Models

		$\Delta G°$ THF solution[b]				
Rxn	$\Delta_r G°$ gas[a]	SSC(V)PE	SM8	COSMO G03	COSMO ADF	exp
$Et_3N + BH_3NH_3 \rightarrow Et_3NBH_3 + NH_3$	−6.6	−3.0	1.5	−4.5	−3.3	1.0 ± 0.1
$Et_3N + BH_3NH_3 \rightarrow [Et_3NBH_3NH_3]^‡$	17.6	24.9	27.9	27.3	25.5	27 ± 2
$BH_3 + THF \rightarrow THFBH_3$	−10.3	−15.9	−16.4	−13.2	−15.8	−16.0[c]

[a] Calculated at G3(MP2)B3LYP for species at 1 atm and 298 K having the following symmetries: Et_3N (C_3), NH_3BH_3 (C_{3v}), Et_3NBH_3 (C_1), NH_3 (C_{3v}), TS (C_1). [b] Solvation models same as Table 4; values include standard state corrections that add 1.89 kcal/mol to ΔG_s* of each reactant/product to account for process of changing from 1 atm gas phase standard state to 1 M solution standard state, except 3.38 kcal/mol is added to ΔG_s* THF to account for process of changing from 1 atm standard state to liquid standard state (mole fraction = 1). [c] Reaction is $BH_3(g) + THF(l) \rightarrow THFBH_3(soln)$ from ref 50 and BE of diborane gas.[29c].

which electrostatic solvation energies differ by as much as 4.4 kcal/mol. However, the models differ considerably in their estimate of the non-electrostatic contributions. The contributions are small in the SM8 and COSMO-ADF models. The COSMO-G03 model predicts the non-electrostatic contributions to be particularly large for Et_3N (6 kcal/mol), Et_3NBH_3 (8 kcal/mol), and $[Et_3NBH_3NH_3]^‡$ (11 kcal/mol) such that their solvation in THF is predicted to be much less favorable compared with the other models. The solvation of Et_3N is predicted to be unfavorable by 4 kcal/mol using the COSMO-G03 parameters. The models tend to predict the boron-containing compounds to have more negative solvation free energies with NH_3BH_3 having the most negative of all, consistent with its large dipole moment and size. The solubility of NH_3BH_3 in THF is high (25 g/100 g THF), and the vapor pressure of NH_3BH_3(c) is extremely low ($\sim 3 \times 10^{-7}$ bar)[65] such that ΔG_s* of transfer from gas to THF solution (mole fraction ~0.6) may be estimated as −12 kcal/mol. However, the high concentration of the saturated solution surely results in NH_3BH_3−NH_3BH_3 interactions so this value is not directly comparable to the calculated ΔG_s* values, which represent solutions at infinite dilution in which NH_3BH_3 interacts only with THF. The dimerization energy of the head−tail dimer of NH_3BH_3 in the gas phase is predicted to be −14.0 kcal/mol at the CCSD(T)/aug-cc-pVTZ + ZPE level.[66]

In Table 5, we compare the calculated free energies of reaction and activation with experimental values. The calculated values are obtained by combining the G3-(MP2)B3LYP gas phase energies (Table 1) for the processes with solvation free energies (Table 4) and standard state corrections.[67] Compared to experiment, the SM8 model overestimates the free energy of reaction 3 by less than 0.5 kcal/mol, SSC(V)PE underestimates it by 4 kcal/mol, and the COSMO models underestimate it by 4−5 kcal/mol. That SM8 agrees best may be traced to it finding solvation of NH_3BH_3 and NEt_3 to be more favorable as compared to the COSMO models. With respect to the free energy of activation, the models calculate values falling within the uncertainty of the experimental value. Thus, calculations of the free energy of activation appear to benefit from some cancellation of errors with the SSC(V)PE and COSMO models deriving the most benefit. The results are consistent with experiment, showing the TS to be less well solvated than the reactants leading to $\Delta S^‡ > 0$. For reaction 6 in which BH_3(g) reacts with THF liquid to form $THFBH_3$ in solution, the SM8 and SSC(V)PE models give $\Delta G_6°$ to within the experimental error of the measured value.

Since the SM8 model gives the more consistent results for the solution reaction free energies in Table 5, we used it to investigate the two-step mechanism depicted by reactions 4 and 5. Reaction free energies and barriers are presented schematically in Figure 2 and compared with the 1-step process reaction 3, all calculated at the SM8/B3LYP/6-31G*//G3(MP2)B3LYP level of theory. Standard state corrections were applied as before for Table 5.[67,68] The two TSs, $[H_3NBH_3THF]^‡$ and $[Et_3NBH_3THF]^‡$, have B−N bond distances of 2.56 Å, which are longer by ~0.25 Å than the B−N distances in $[H_3NBH_3NEt_3]^‡$. The B−O distances are 1.99 and 2.10 Å, respectively. Thus, consistent with Hammond's postulate,[69] the TSs lie closer to $THFBH_3$ on

(65) Dedrick, D. E.; Behrens, R.; Kanouff, M. *Sandia National Laboratories Hydrogen Storage Development Program Quarterly Progress Report for July-September, 2008*; Sandia National Laboratories: Livermore, CA, 2008.

(66) Nguyen, V. S.; Matus, H.; Grant, D. J.; Nguyen, M. T.; Dixon, D. A. *J. Phys. Chem A.* **2007**, *111*, 8844.

(67) We applied a correction of 1.89 kcal/mol to ΔG_s* to represent the process of changing from a gas at 1 atm to a solution with a solute concentration of 1 M.[51]

(68) We applied a correction of 3.38 kcal/mol to ΔG_s* to represent the process of changing THF from a gas at 1 atm to a liquid (mole fraction = 1).

(69) Hammond, G. S. *J. Am. Chem. Soc.* **1955**, *77*, 334–338.

the reaction coordinate than to either NH_3BH_3 or Et_3NBH_3. The calculated $\Delta G_r°$ in the gas phase (1 atm, 298 K) for the overall reaction 3 is −6.6 kcal/mol. However, substitutions of THF on NH_3BH_3 and Et_3NBH_3 are disfavored by 7.3 and 13.9 kcal/mol to form the $THFBH_3$ complex, respectively. From Figure 2 it is apparent that the one-step S_N2 path presents the lower barrier for substitution of Et_3N on NH_3BH_3 in the solution phase (as well as the gas phase). In the gas (solution) phase, the free energy of $[THFBH_3NEt_3]^‡$ on the 2-step reaction path is 1.3 (2.9) kcal/mol greater than that of $[Et_3NBH_3NH_3]^‡$ on the 1-step reaction path, According to this analysis, reaction 4, THF substitution on NH_3BH_3, is competitive with reaction 3, Et_3N substitution, when concentrations of Et_3N are less than ~1 *M*. *However, if the difference in barriers between reactions* (5) *and* (3) *is ~3 kcal/mol, then the 1-step path should dominate when* $[Et_3N] \geq 0.006$ *and the concentration of ammonia is sufficiently high to make the reverse of reaction* (4) *faster than reaction* (5) (*e.g.*, $[NH_3]/[Et_3N] > 0.003$).

Materials and Methods

General Experimental Procedures. All reactions were conducted under inert atmosphere following techniques described by Shriver and Drezdon.[70] THF was purified by passage through activated alumina using an Inovative Technology, Inc. PureSolv solvent purification system. $THFBH_3$ was purchased from Aldrich chemical and molarity determined by monitoring the standard addition of Ph_3BH_3 by ^{11}B NMR spectroscopy. Triethylamine was purchased from Aldrich Chemical Co. and purified by distillation over calcium hydride followed by several freeze−pump−thaw cycles. High purity ammonia borane was purchased from Aviabor Inc. and used without further purification. Additional details are given in the Supporting Information.

Preparation and Calorimetry of LBH_3 Adducts in THF. Heats of reaction of $THFBH_3$ with select Lewis bases were measured using a Calvet differential scanning calorimeter, DSC C80, operating in the isothermal mode. Reactions were conducted in a stainless steel Hastealloy mixing cell at 25 °C. Percent conversion was verified by ^{11}B NMR spectroscopy and conditions adjusted to achieve 98−100% conversion to desired product. All reactions were complete within 2 h of mixing. Exact masses and volumes for reagents and solvents for each reaction are listed in the Supporting Information. ***Caution!*** *Note that pyridine BH_3 is thermally unstable*[71] *and should be handled with care. It ignited unpredictably with a bright green flame when exposed to air.*

Characterization of Adducts. LBH_3 adducts prepared in the calorimeter were monitored by ^{11}B NMR afterward to ensure that 100% conversion had occurred. Most adducts have been reported previously. ^{11}B chemical shifts were compared to chemical shifts of authentic samples in THF and previously reported[72] ^{11}B NMR spectra recorded in THF.

Kinetics. Measurements were made on reactions run in sealed medium-walled quartz NMR tubes filled to ~95% of the total tube volume to ensure negligible concentration of NH_3 in the gas phase. Reactions were kept in constant temperature baths between measurements. ^{11}B NMR spectra were recorded on a Varian Inova 500 MHz instrument operating at 160 MHz. Starting with NH_3BH_3, the increase in Et_3NBH_3 was determined by ^{11}B NMR and fit by numerically integrating the reversible second order rate law. Fits to reaction 3 were performed using pro Fit version 6.1,[73] and fits to eqs 4 and 5 were performed using Berkeley Madonna, version 8.3.[74]

Computational Methods. Electronic structure calculations using the NWChem package of programs[75] were performed to predict the thermochemistry of the Lewis base adducts to BH_3 at MP2[76] and DFT[77] levels of theory given in Table 1. Minimum energy structures were optimized using DFT with the B3LYP exchange-correlation functional[78] and 6-311+G** basis set.[79] Single point energies for optimized geometries were calculated at the MP2/aug-cc-pVTZ level. Minimum energy geometries were confirmed to be bound states by the absence of imaginary frequencies, and transition states were confirmed by the presence of exactly one imaginary frequency. Enthalpies and free energies at 298 K of optimized structures were calculated from frequency calculations using the harmonic oscillator-rigid-rotor approximation with entropies corrected for rotational symmetry number.[80] G3(MP2)[81] and G3(MP2)B3LYP[82] calculations were performed using the Gaussian-98[83] and Gaussian-03 packages.[57] Continuum solvation models, SM8[52] in GAMESSPLUS[53] and SSC(V)PE[54] in HONDO version 06.10[55] and COSMO (Gaussian-03[57] and ADF[58]), were used to calculate solvation free energies in THF without reoptimizing the gas phase geometries. For the COSMO (B3LYP/DZVP2) calculations in Gaussian-03, the radii developed by Klamt and coworkers were used to define the cavity.[56] For the COSMO calculations (B88P86/TZ2P)[84] in ADF, the default MM3 radii from Allinger and co-workers[85] were used to define the cavity. Cartesian coordinates of all calculated compounds reported in this work are listed in the Supporting Information.

For the As compounds, it is currently not possible to perform G3(MP2) calculations so a slightly different approach was used. The energy of AsH_3 and AsH_3BH_3 were calculated at the CCSD(T) level[86−88] with the augmented correlation consistent basis sets aug-cc-pV*n*Z[89] for H and B and

(70) Shriver, D. F.; Drezdon, M. A. *Manipulations of Air Sensitive Compounds*, 2nd ed.; Wiley: New York, 1968.

(71) Lane, C. L. *Ammonia-Borane and Related N-B-H Compounds and Materials: Safety Aspects, Properties and Applications* (*A survey completed as part of a project for the DOE Chemical Hydrogen Storage Center of Excellence, Contract # DE-FC36−05GO15060*); Northern Arizona University: Flagstaff, AZ, 2006. (www1.eere.energy.gov/hydrogenandfuelcells/pdfs/nbh_h2_storage_survey.pdf)

(72) (a) Me_3PBH_3: Heitsch, C. W. *Inorg. Chem.* **1965**, *4*, 1019. (b) Ph_3PBH_3: Graybill, B. M.; Ruff, J. K. *J. Am. Chem. Soc.* **1962**, *84*, 1062. (c) Me_2SBH_3: Brown, H. C.; Ravindran, N. *Inorg. Chem.* **1977**, *16*, 2938. (d) $PyBH_3$: Onak, T. P.; Landesman, H.; Willams, R. E.; Shapiro, I. *J. Phys. Chem.* **1959**, *63*, 1533. (e) Et_3NBH_3: Brown, H. C.; Sikorski, J. A. *Organometallics* **1982**, *1*, 28.

(73) *pro Fit*, ver 6.1; QuantumSoft: Bühlstr. 18, CH-8707 Uetikon am See, Switzerland; www.quansoft.com/index.html.

(74) Macey, R. I.; Oster, G. F. *Berkeley Madonna*, version 8.3; http://www.berkeleymadonna.com/

(75) Bylaska, E. J. et al.; *NWChem, A Computational Chemistry Package for Parallel Computers*, Version 5.0; Pacific Northwest National Laboratory: Richland, WA, 2006.

(76) (a) Møller, C.; Plesset, M. S. *Phys. Rev.* **1934**, *46*, 618. (b) Pople, J. A.; Binkley, J. S.; Seeger, R. *Int. J. Quantum Symp.* **1976**, *10*, 1.

(77) (a) Hohenberg, P.; Kohn, W. *Phys. Rev.* **1964**, *136*, B864. (b) Kohn, W.; Sham, L. J. *Phys. Rev.* **1965**, *140*, A1133.

(78) (a) Becke, A. D. *J. Chem. Phys.* **1993**, *98*, 5648. (b) Lee, C.; Yang, W.; Parr, R. G. *Phys. Rev. B* **1988**, *37*, 785.

(79) Schafer, A.; Huber, C.; Ahlrichs, R. *J. Chem. Phys.* **1994**, *100*, 5829.

(80) Fernández-Ramos, A.; Ellingson, B.; Meana-Pañeda, R.; Marques, J.; Truhlar, D. *Theor. Chem. Acc.* **2007**, *118*, 813–826.

(81) Curtiss, L. A.; Redfern, P. C.; Raghavachari, K.; Rassolov, V.; Pople, J. A. *J. Chem. Phys.* **1999**, *110*, 4703.

(82) Baboul, A. G.; Curtiss, L. A.; Redfern, P. C.; Raghavachan, K. *J. Chem. Phys.* **1999**, *110*, 7650.

(83) Frisch, M. J.; et al. *Gaussian 98*, Revision A.11.4; Gaussian, Inc.: Pittsburgh, PA, 2002.

(84) Becke, A. D. *Phys. Rev. A* **1988**, *38*, 3098. Perdew, J. P. *Phys. Rev. B* **1986**, *33*, 8822.

(85) Allinger, N. L.; Yuh, Y. H.; Lii, J. H. *J. Am. Chem. Soc.* **1989**, *111*, 8551. Lii, J. H.; Allinger, N. L. *J. Am. Chem. Soc.* **1989**, *111*, 8566; 8576.

(86) Purvis, G. D., III; Bartlett, R. J. *J. Chem. Phys.* **1982**, *76*, 1910.

(87) Raghavachari, K.; Trucks, G. W.; Pople, J. A.; Head-Gordon, M. *Chem. Phys. Lett.* **1989**, *157*, 479.

(88) Watts, J. D.; Gauss, J.; Bartlett, R. J. *J. Chem. Phys.* **1993**, *98*, 8718.

(89) Kendall, R. A.; Dunning, T. H.; Harrison, R. J. *J. Chem. Phys.* **1992**, *96*, 6796.

aug-cc-pV*n*Z-PP[90] for As with n = D, T, and Q at the B3LYP/DZVP geometries.[91] The open shell atomic energies were done in the R/UCCSD(T) formalism.[92−94] The CCSD(T) energies were extrapolated to the CBS limit by fitting to a mixed Gaussian/exponential equation:

$$E(n) = E_{CBS} + A \exp[-(n-1)] + B \exp[-(n-1)^2]$$

with n = 2, 3, and 4 giving the CBS-DTQ values as first proposed by Peterson et al.[95] Core−valence corrections were calculated at the CCSD(T) level with the aug-cc-pVTZ basis set for H, aug-cc-pwCVTZ basis set for B, and aug-cc-pwCVTZ-PP basis set for As.[96] Scalar relativistic corrections were calculated as the expectation values of the mass-velocity and Darwin operators (MVD) from the Breit-Pauli Hamiltonian[97] for the CISD (configuration interaction with single and double excitations) wave function with the aT basis set. The atomic spin−orbit corrections (SO) were obtained from the experimental values for the ground states of the atoms (−0.03 for B and 0 kcal/mol for H and As).[98] Zero point energies were taken from B3LYP/DZVP calculations with scale factors of 0.986 for the As−H stretches[99] and 0.982 for the B−H stretches.[100−102] The total atomization energies (TAEs) at 0 K were calculated from eq 7.

$$\sum D_{0,0K} = \Delta E_{CBS} + \Delta E_{SR} + \Delta E_{CV} + \Delta E_{ZPE} + \Delta E_{SO} \quad (7)$$

Heats of formation at 0 K for AsH_3, BH_3, and AsH_3BH_3 were calculated from the above calculated TAEs and the heats of formation of the atoms at 0 K (51.63 kcal/mol for H,[103] 135.10 kcal/mol for B,[104] and 68.37 kcal/mol for As). The As value is derived from the bond dissociation energy of As_2 of 91.01 kcal/mol at 0 K obtained at the same composite CCSD(T)/CBS level and the heat of formation of As_2 of 45.73 kcal/mol at 0 K obtained from the 298 K heat of formation of Rau[105] and the thermal correction of Wagman et al.[106] This heat of formation differs from the heat of formation of As given by Wagman et al.[106] of 72.0 kcal/mol by 3.6 kcal/mol. Heats of formation at 298 K were calculated by following the procedures outlined by Curtiss et al.[107] The CCSD(T) calculations were performed with the MOLPRO program package.[108] This approach follows one that some of us have been developing with Washington State University for the prediction of the heats of formation of a wide range of compounds.[109,110] The calculated heat of formation of AsH_3 using the new value for $\Delta H_{f,0}$(As) differs from the experimental value[106,111] of 15.87 ± 0.25 kcal/mol by only 1.1 kcal/mol, type of error expected for such calculations. Use of the Wagman et al.[106] value for $\Delta H_{f,0}$(As) gives $\Delta H_{f,298}(AsH_3)$ = 20.6 kcal/mol, an error of almost 5 kcal/mol which is far outside our confidence limits in the calculations. Given the heats of formation of AsH_3, BH_3, and AsH_3BH_3, one can calculate the As−B bond dissociation energy. The As−B bond energy for a substituted arsine can then be calculated relative to the higher-level value from the following reaction

$$AsH_3BH_3 + AsR_3 \rightarrow AsR_3BH_3 + AsH_3 \quad (8)$$

The energy for reaction 8 was calculated at the MP2 level with the aug-cc-pV*n*Z+aug-cc-pV*n*Z-PP level with n = D for R = phenyl and for n = T for R = ethyl using geometries optimized at the B3LYP/DZVP level.

Conclusion

Displacement reactions involving Lewis base adducts of BH_3 are important for a variety of different synthesis and energy storage applications. In this study the thermochemistry and kinetics of forming Lewis base adducts of BH_3 were investigated both experimentally and computationally in solution and gas phase. G3MP2 methods using either the MP2 or the B3LYP geometries give dative bond energies that are in agreement with the few available experimental data and reproduce benchmark CCSD(T)/CBS results usually to within ~1 kcal/mol. Measured heats of displacement of $THFBH_3$ by Et_3N and NH_3 in THF are similar. The kinetics of substitution on boron of BH_3NH_3 by Et_3N were measured in THF solution and found to fit well to a reversible second order rate equation with Arrhenius parameters: log A = 14.7 ± 1.1 and E_a = 28.1 ± 1.5 kcal/mol. The kinetic data are consistent with a one-step S_N2 displacement of NH_3 from NH_3BH_3 with Et_3N. The reaction was then modeled in both gas and solution phase to gain a better understanding of the reaction mechanism. Dielectric continuum solvation models were surveyed to identify the optimum model chemistry for Lewis base BH_3 displacement reactions. The SM8 model chemistry accurately reproduces the measured reaction thermochemistry and kinetics, overestimating the free energies of reaction and activation by less than 0.5 kcal/mol. The solution phase barrier to the S_N2 reaction is similar in energy to the gas phase dissociation energy of ammonia borane; however, a stepwise mechanism involving solvent-assisted dissociation

(90) (a) Peterson, K. A. *J. Chem. Phys.* **2003**, *119*, 11099. (b) Peterson, K. A.; Figgen, D.; Goll, E.; Stoll, H.; Dolg, M. *J. Chem. Phys.* **2003**, *119*, 11113.
(91) Godbout, N.; Salahub, D. R.; Andzelm, J.; Wimmer, E. *Can. J. Chem.* **1992**, *70*, 560.
(92) Rittby, M.; Bartlett, R. J. *J. Phys. Chem.* **1988**, *92*, 3033.
(93) Knowles, P. J.; Hampel, C.; Werner, H.-J. *J. Chem. Phys.* **1994**, *99*, 5219.
(94) Deegan, M. J. O.; Knowles, P. J. *Chem. Phys. Lett.* **1994**, *227*, 321.
(95) Peterson, K. A.; Woon, D. E.; Dunning, T. H., Jr. *J. Chem. Phys.* **1994**, *100*, 7410.
(96) Peterson, K. A.; Dunning, T. H., Jr. *J. Chem. Phys.* **2002**, *117*, 10548. Woon, D. E.; Dunning, T. H., Jr. *J. Chem. Phys.* **1993**, *98*, 1358.
(97) Davidson, E. R.; Ishikawa, Y.; Malli, G. L. *Chem. Phys. Lett.* **1981**, *84*, 226.
(98) Moore, C. E. *Atomic Energy Levels as Derived from the Analysis of Optical Spectra, Vol. 1, H to V*; U.S. National Bureau of Standards Circular 467; U.S. Department of Commerce, National Technical Information Service, COM-72−50282: Washington, D C, 1949.
(99) Shimanouchi, T. *Tables of Molecular Vibrational Frequencies, Consolidated Volume 1*; NSRDS NBS-39, **1972**.
(100) Jacox, M. E. *J. Phys. Chem. Ref. Data* **1994**, Monograph 3.
(101) (a) Duncan, J. L.; Mills, I. M. *Spectrochim. Acta* **1964**, *20*, 523. (b) Hoy, A. R.; Mills, I. M.; Strey, G. *Mol. Phys.* **1972**, *24*, 1265.
(102) Kawaguchi, K.; Butler, J. E.; Bauer, S. H.; Minowa, T.; Kanamori, H.; Hirota, E. *J. Chem. Phys.* **1992**, *96*, 3411.
(103) Chase, M. W., Jr. *NIST-JANAF Thermochemical Tables*, 4th ed.; *J. Phys. Chem. Ref. Data, Mono. 9*; American Institute of Physics: Woodbury, NY, 1998; Suppl 1.
(104) Karton, A.; Martin, J. M. L. *J. Phys. Chem. A* **2007**, *111*, 5936.
(105) Rau, H. *J. Chem. Thermodyn.* **1975**, *7*, 27.
(106) Wagman, D. D.; Evans, W. H.; Parker, V. B.; Schumm, R. H.; Halow, I.; Bailey, S. M.; Churney, K. L.; Nuttall, R. L. *J. Phys. Chem. Ref. Data* **1982**, *11* (Suppl. 2).
(107) Curtiss, L. A.; Raghavachari, K.; Redfern, P. C.; Pople, J. A. *J. Chem. Phys.* **1997**, *106*, 1063.
(108) Werner, H.-J. et al. *MOLPRO, a package of ab initio programs*, version 2006.1; see http://www.molpro.net.
(109) (a) Feller, D.; Dixon, D. A. *J. Phys. Chem. A* **2000**, *104*, 3048. (b) Feller, D.; Dixon, D. A. *J. Chem. Phys.* **2001**, *115*, 3484. (c) Dixon, D. A.; Feller, D.; Peterson, K. A. *J. Chem. Phys.* **2001**, *115*, 2576. (d) Ruscic, B.; Wagner, A. F.; Harding, L. B.; Asher, R. L.; Feller, D.; Dixon, D. A.; Peterson, K. A.; Song, Y.; Qian, X.; Ng, C.; Liu, J.; Chen, W.; Schwenke, D. W. *J. Phys. Chem. A* **2002**, *106*, 2727. (e) Feller, D.; Dixon, D. A. *J. Phys. Chem. A* **2003**, *107*, 9641. (f) Dixon, D. A.; Gutowski, M. *J. Phys. Chem. A* **2005**, *109*, 5129. (g) Pollack, L.; Windus, T. L.; de Jong, W. A.; Dixon, D. A. *J. Phys. Chem. A* **2005**, *109*, 6934. (h) Dixon, D. A.; Grant, D. J.; Christe, K. O.; Peterson, K. A. *Inorg. Chem.* **2008**, *47*, 5485. (i) Dixon, D. A.; Grant, D. J.; Peterson, K. A.; Christe, K. O.; Schrobilgen, G. J. *Inorg. Chem.* **2008**, *47*, 5485. (j) Grant, D. J.; Dixon, D. A.; Francisco, J. S.; Feller, D.; Peterson, K. A. *J. Phys. Chem. A* **2009**, *113*, 11343.
(110) Feller, D.; Peterson, K. A.; Dixon, D. A. *J. Chem. Phys.* **2008**, *129*, 204015.
(111) Gunn, S. R.; Jolly, W. L.; Green, L. G. *J. Phys. Chem.* **1960**, *64*, 1334.

was modeled and found to be 3 kcal/mol less favorable consistent with the reaction proceeding primarily by a classical S_N2 mechanism. Thermochemical and kinetic data suggest Et_3N to be a suitable carrier for borane in an ammonia borane chemical regeneration process because of the thermal stability of Et_3NBH_3 and favorable thermochemistry for substitution with NH_3 in solution.

Acknowledgment. This work was funded by the Department of Energy, Office of Energy Efficiency and Renewable Energy under the Hydrogen Storage Grand Challenge, Solicitation No. DE-PS36-03GO93013. This work was done as part of the Chemical Hydrogen Storage Center. D.A.D. also thanks the Robert Ramsay Chair Fund of The University of Alabama for support. A portion of this work was performed using the Molecular Sciences Computing Facility (MSCF) at EMSL, a national scientific user facility sponsored by the Department of Energy's Office of Biological and Environmental Research and located at Pacific Northwest National Laboratory.

Supporting Information Available: Details of calorimetric and kinetic measurements, computational methods, including computed thermochemical values and geometries. This material is available free of charge via the Internet at http://pubs.acs.org.

Note Added after ASAP Publication. This paper was posted on October 8, 2010. It was reposted on October 18, 2010, with a number of text corrections and a new Supporting Information file.